

# Optics Letters

## Frequency-modulated microwave generation with feedback stabilization using an optically injected semiconductor laser

JUN-PING ZHUANG,<sup>1</sup> XIAO-ZHOU LI,<sup>1</sup> SONG-SUI LI,<sup>1</sup> AND SZE-CHUN CHAN<sup>1,2,\*</sup>

<sup>1</sup>Department of Electronic Engineering, City University of Hong Kong, Hong Kong, China

<sup>2</sup>State Key Laboratory of Millimeter Waves, City University of Hong Kong, Hong Kong, China

\*Corresponding author: scchan@cityu.edu.hk

Received 1 November 2016; revised 21 November 2016; accepted 21 November 2016; posted 21 November 2016 (Doc. ID 279845); published 12 December 2016

**Generation of frequency-modulated continuous-wave (FMCW) microwave signals is investigated using the period-one (P1) dynamics of a semiconductor laser. A modulated optical injection drives the laser into P1 oscillation with a modulated microwave frequency, while adding feedback to the injection reduces the microwave phase noise. Using simply a single-mode laser, the tunability of P1 dynamics allows for wide tuning of the central frequency of the FMCW signal. A sweep range reaching 7.7 GHz is demonstrated with a sweep rate of 0.42 GHz/ns. When the external modulation frequency matches the reciprocal of the feedback delay time, feedback stabilization is manifested as an increase of the frequency comb contrast by 30 dB for the FMCW microwave signal.** © 2016 Optical Society of America

**OCIS codes:** (350.4010) Microwaves; (250.5960) Semiconductor lasers; (140.3520) Lasers, injection-locked.

<https://doi.org/10.1364/OL.41.005764>

Photonic generation of microwave waveforms as a modulation on an optical carrier has been widely investigated due to the capabilities of low-loss delivery over optical fibers and the possibility of exceeding the bandwidth limitations of electronics [1–5]. Among the waveforms generated, frequency-modulated continuous-wave (FMCW) microwave signals in the form of sinusoids with time-varying microwave frequencies have received particular attention [6–9]. The instantaneous frequencies of an FMCW microwave signal measured at the source and the detector allow the determination of the round-trip delay of propagation. Thus FMCW signals have been commonly utilized in ranging, imaging, and communication applications [6,9]. A number of approaches have been developed for generating photonic microwave FMCW signals. Some approaches directly adopt electro-optic intensity modulators that are fed by CW lasers, but the generation of the FMCW signals is based on electronic voltage-controlled oscillators, which typically have small electronic bandwidths in limiting the frequency sweep ranges and sweep rates to the orders of 1 GHz and 0.01 GHz/ns, respectively [6,10,11]. Variant approaches using

injection-locking of lasers allow extension of the sweep ranges [12]. Alternatively, photonic microwave FMCW signals can be generated using femtosecond mode-locked pulses through spectral shaping in combination with wavelength-to-time mapping [7–9]. The central frequency and sweep range are fixed unless the pulse shaper is thermally adjusted or reconfigured otherwise. In addition, tunable FMCW microwave signals also can be generated by heterodyning a CW laser with a wavelength-swept laser that is carefully controlled by sweeping the bias current [13]. The optical phase fluctuations between the two independent lasers are translated to the phase noise in the FMCW signals, which necessitates fast optical phase-locked loops to accurately stabilize the lasers [14].

Recently, tunable photonic microwave generation has been investigated based on the period-one (P1) oscillation in semiconductor lasers [3–5,15–21]. The P1 oscillation is a form of nonlinear dynamics in a single-mode semiconductor laser subject to a constant optical injection. The injection causes the undamping of the relaxation resonance, forcing the laser to trace a limit-cycle trajectory, which yields a sustained intensity oscillation at a single-tone microwave frequency [4,16]. Such a P1 oscillation of the intensity offers many advantages in photonic microwave generation, including a wide frequency tunability spanning up to 100 GHz [20,22], large intensity modulation depth approaching unity [15,23], and flexible variation between single- and double-sided optical spectra [24]. The P1 oscillation inherently contains phase noise that can be suppressed by methods such as optical feedback, optoelectronic feedback, and low-sensitivity operation [4,5,25,26]. The P1 oscillation hence has been demonstrated for a number of applications, including radio-over-fiber communication [27], amplitude-to-frequency modulation format conversion [28], frequency multiplication [21,29], and photonic microwave amplification [30]. However, the generation of FMCW signals has yet to be explored using the P1 oscillation through incorporating modulation on its microwave frequency.

In this Letter, FMCW microwave signal generation is experimentally demonstrated based on the P1 oscillation of an optically injected semiconductor laser. A constant injection

first drives the laser into P1 oscillation at a fixed microwave frequency. An external modulation on the injection then modulates the P1 oscillation in yielding an FMCW signal. Delayed feedback is further applied through the injection for phase noise reduction. The resultant FMCW signal has a tunable central frequency  $f_0$  due to the wide tunability of P1 oscillation. The sweep range  $\Delta f$  can be easily adjusted by the modulation index on the injection. The phase noise is effectively reduced by matching the external modulation frequency  $f_m$  to the reciprocal of the feedback delay time  $\tau$ . Experimentally, the P1 oscillation generates FMCW microwave signals with a central frequency tunable well beyond the relaxation resonance frequency, a sweep range reaching 7.7 GHz, and a sweep rate of up to 0.42 GHz/ns. Phase noise reduction by using feedback stabilization is manifested as a significant improvement of the frequency comb contrast  $R$  by 30 dB in the power spectrum of the FMCW signal.

Figure 1 shows the experimental schematic for an FMCW microwave signal generation based on P1 oscillation. Two lasers are arranged in a master–slave configuration for modulated optical injection. The slave laser is a 1.55- $\mu\text{m}$  distributed-feedback single-mode semiconductor laser (Nortel LC111-18) packaged with a fiber pigtail. It is temperature-controlled at 20°C and electrically biased at 60 mA, which is above the threshold of 25 mA. The laser emits about 2.0 mW through the fiber at position  $T$ . Its relaxation resonance frequency is about 7 GHz. The master laser (HP 8168A) emits CW light that passes through an erbium-doped fiber amplifier A (Amonics AEDFA-23-B-FA), a Mach–Zehnder modulator MZM (Covega Mach-10), and an optical circulator for injecting into the slave laser. The optical injection power  $P_i$  at position  $T$  is controlled by the gain of the fiber amplifier A. The optical detuning frequency  $f_i$  of the CW injection light, in reference to the free-running optical frequency of the slave laser, is controlled at the master laser [22]. The polarizations of the injection light, MZM, and slave laser are matched by adjusting polarization controllers PC1 and PC2. MZM has an electrical bandwidth of 12 GHz and a quarter-wave voltage  $V_{\pi/2}$  of 2.2 V. It is biased at quadrature by a voltage  $V_{\text{DC}}$  for a non-inverting linear operation through its low-frequency electrode.

When MZM is electrically disconnected from other inputs in Fig. 1, the CW optical injection from the master laser is sufficient to drive the slave laser into P1 oscillation, so the emission intensity of the slave laser oscillates at a microwave frequency  $f_0$  tunable by the injection parameters  $(P_i, f_i)$  [4,22]. The emission of the slave laser is transmitted through the circulator, a 50:50 fiber coupler FC, and a photodetector PD1 comprising of a detector ( $u^2t$  XPDV2120RA) and an amplifier that gives an overall conversion efficiency of 5 A/W. The output obtained after PD1 is monitored by a power spec-

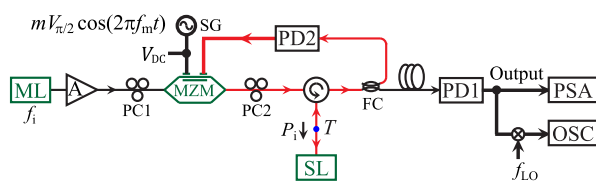


**Fig. 1.** FMCW microwave signal generation using a semiconductor laser in P1 oscillation by modulated optical injection with feedback. ML, master laser; SL, slave laser; SG, signal generator; PSA, power spectrum analyzer; OSC, oscilloscope.

trum analyzer (Agilent N9010A) and a real-time oscilloscope (Agilent 90254A). The oscilloscope only covers the baseband of up to 2.5 GHz, so a microwave mixer with a local oscillator at frequency  $f_{\text{LO}}$  is adopted for downconversion. As an illustration, Fig. 2(a) shows the optical spectrum of the emission of the slave laser measured immediately before PD1 when the injection parameters are set at  $(P_i, f_i) = (0.6 \text{ mW}, 2.1 \text{ GHz})$ . The horizontal axis is offset to the free-running optical frequency of the slave laser for reference. The arrow at the offset of  $f_i$  indicates the optical frequency component regenerated from the optical injection [22]. The P1 dynamics generates the optical sidebands equally separated by the P1 oscillation frequency  $f_0$  [16]. These sidebands beat at PD1 in yielding the black power spectrum in Fig. 2(b), which peaks at the generated  $f_0 = 10 \text{ GHz}$ , where a 3-dB linewidth of 1.9 MHz is observed due to phase noise associated with the oscillation.

Then MZM is externally modulated by connecting its low-frequency electrode to an electrical signal generator in Fig. 1 with a time-varying voltage  $mV_{\pi/2} \cos(2\pi f_m t)$ , where  $f_m$  and  $m$  are the modulation frequency and modulation index, respectively. The injection optical power from the master laser is modulated by MZM, causing a modulation of the refractive index of the slave laser through the anti-guidance effect, which, in turn, modulates the cavity resonance frequency [16,28,31]. This results in a frequency modulation of the P1 oscillation in generating an FMCW microwave output signal. Additionally, an electrical feedback to MZM can be formed by connecting its high-frequency electrode to the upper port of the fiber coupler through an amplified photodetector PD2, which comprises of an AC-coupled photodetector (Newport AD-10ir) and a microwave amplifier (Agilent 83006A). The feedback loop is highlighted in red in Fig. 1, where its round-trip delay time  $\tau$  is about 56 ns for a modulation signal to propagate from MZM, entering and exiting the slave laser, through the fiber coupler and PD2, and then returning to MZM. Both implemented through MZM, the external modulation is responsible for generating the FMCW signal, whereas the feedback is responsible for phase noise reduction.

Figure 3 shows the FMCW microwave signal generated when the P1 oscillation is subject to a modulated optical injection with  $(m, f_m) = (0.09, 17.84 \text{ MHz})$ , where the feedback at PD2 is disconnected and connected in columns (i) and (ii), respectively. The master laser remains unchanged so that the time-averaged injection power  $P_i$  is maintained at 0.6 mW with detuning frequency  $f_i = 2.1 \text{ GHz}$ . In Fig. 3(a-i), the emission intensity time series of the slave laser is recorded by the oscilloscope after downconversion by the local oscillator at  $f_{\text{LO}} = 8.8 \text{ GHz}$ . The downconverted signal is a sinusoid with an instantaneous microwave frequency that continuously sweeps between 0.4 and 1.9 GHz. Thus the original output

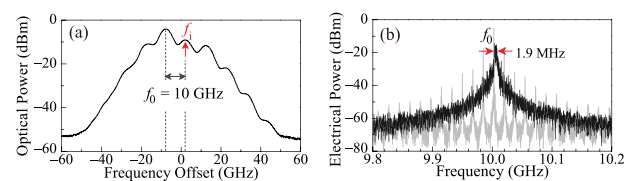


**Fig. 2.** (a) Optical spectrum and (b) power spectrum of the emission from the slave laser under CW optical injection. Injection parameters are fixed at  $(P_i, f_i) = (0.6 \text{ mW}, 2.1 \text{ GHz})$ . Optical resolution bandwidth: 7.5 GHz. Electrical resolution bandwidth: 100 kHz.

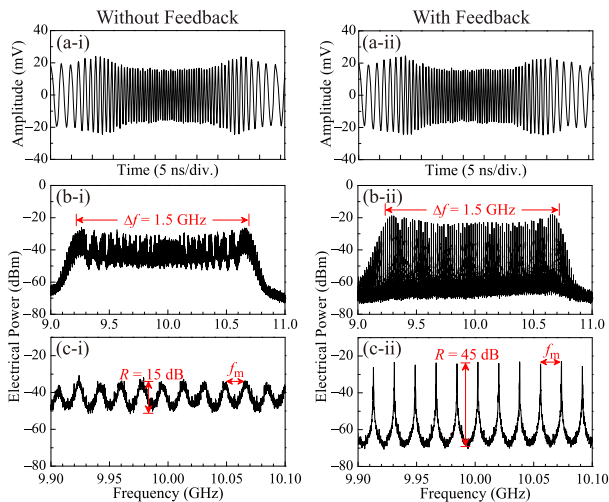


**Fig. 3.** (a) Intensity time series, (b) power spectrum, and (c) zoomed power spectrum of the FMCW emission from the slave laser under modulated optical injection. The feedback from PD2 to MZM is (i) disconnected and (ii) connected. The time series is measured at the oscilloscope after the output from PD1 is downconverted. The modulation parameters are set at  $(m, f_m) = (0.091, 17.84 \text{ MHz})$ .

signal generated at PD1 is an FMCW signal that sweeps between 9.2 and 10.7 GHz. The frequency sweep repeats in every cycle of  $1/f_m$ , though only one cycle is plotted in Fig. 3(a-i). In Fig. 3(b-i), the corresponding power spectrum clearly shows the generated frequencies spanning from 9.2 to 10.7 GHz, which gives a sweep range of  $\Delta f = 1.5$  GHz around a slightly lowered central frequency  $f_0$  of 9.95 GHz. Though an ideal FMCW spectrum should be a frequency comb with components separated by  $f_m$ , the actual spectrum is affected by noisy phase fluctuations of the P1 oscillation. As a zoom in Fig. 3(c-i), the spectrum is plotted in a small frequency span. A periodicity in  $f_m$  is observed with a comb contrast  $R$  of only 15 dB [32], as the spectral peaks have wide linewidths on the order of 1 MHz due to noise.

For noise reduction, feedback stabilization is adopted by connecting PD2 to MZM. The slave laser is thus subject to optical injection that is modulated both by the signal generator at  $f_m$  and the feedback FMCW microwave signal between  $f_0 \pm \Delta f/2$ . The feedback FMCW signal at PD2 has a voltage amplitude of  $0.17V_{\pi/2}$ , which is fixed throughout the experiment. In Fig. 3(a-ii), the time series at the oscilloscope again shows similar sweeping of instantaneous frequency as in Fig. 3(a-i). The slave laser generates the FMCW signal with a sweep range of  $\Delta f = 1.5$  GHz regardless of whether feedback is applied. In Fig. 3(b-ii), however, the power spectrum clearly shows the effect of the feedback stabilization for which sharp frequency comb components separated by  $f_m$  are observed. As for the zoom in Fig. 3(c-ii), the linewidths of the frequency comb components are significantly narrowed by the feedback to about 20 kHz, while the comb contrast is much increased to  $R = 45$  dB. Comparing Figs. 3(c-i) and 3(c-ii), the feedback stabilization effectively increases the comb contrast  $R$  by 30 dB. Such feedback stabilization is possible because the modulation frequency  $f_m$  of 17.84 MHz is carefully set equal to  $1/\tau$ , where the round-trip delay time  $\tau$  of the feedback loop is about 56 ns. On the one hand, the feedback loop

supports microwave modes separated by  $1/\tau$  because it is an optoelectronic cavity for a signal that is represented electrically at the input of the MZM, then optically for entering and exiting the slave laser, and again electrically after PD2 for returning to MZM [33]. On the other hand, the modulated injection gives microwave sidebands separated by  $f_m$  around the central P1 oscillation frequency  $f_0$  of the emission intensity of the slave laser. Because  $f_m$  equals  $1/\tau$ , the microwave sidebands effectively lock the microwave modes of the optoelectronic cavity, resulting in the narrow linewidth frequency comb of the FMCW signal in Fig. 3(b-ii). It is worth noting that the combination of the external modulation and the feedback loop results in a form of Fourier domain mode-locking [34], although the locking is on the microwave modes of the optoelectronic cavity rather than on some conventional external cavity optical modes. For completeness, the gray spectrum in Fig. 2(b) is recorded with feedback when the modulation is turned off. The feedback narrows the linewidth at  $f_0$  to 20 kHz, while microwave modes separated by  $1/\tau$  are observed.

Details of the FMCW output signal are presented in Fig. 4 while keeping the injection and modulation parameters of Fig. 3. The feedback at PD2 is again disconnected and connected, respectively, in columns (i) and (ii) of Fig. 4. Figure 4(a) shows the spectrograms of the FMCW microwave signals at the output of PD1 in Fig. 1. Each spectrogram is a collection of the power spectra collected at different time instances, where the instantaneous electrical spectral power is plotted in color [7,9]. The spectrograms are calculated by applying a 4-ns Gaussian sliding window for a short-time Fourier transformation on the downconverted time series at the oscilloscope, followed by upshifting the frequency axis by  $f_{LO}$ . The spectrograms in Fig. 4(a) reveal sinusoidal variation of the peak instantaneous microwave frequency between  $f_0 \pm \Delta f/2$  over every cycle of  $1/f_m$ , where the central frequency  $f_0 = 9.95$  GHz and sweep range  $\Delta f = 1.5$  GHz are marked. Thus the fastest sweep rate of the instantaneous frequency is  $\pi \Delta f f_m = 0.08 \text{ GHz/ns}$  in Fig. 4(a). The FMCW spectrograms are attributed to modulated injection and are nearly unchanged by the feedback.

Contrarily, as Fig. 4(b) shows, the feedback has significant influences on the microwave phase noise associated with the FMCW signal. Expressing an FMCW microwave signal as  $\cos(2\pi f_0 t + \varphi)$  with the time-varying phase  $\varphi(t) = -(\Delta f/2f_m) \sin(2\pi f_m t) + \Delta\varphi(t)$ , the phase deviation  $\Delta\varphi(t)$  is non-zero, indicating the fluctuations of the central frequency  $f_0$  when there are noisy fluctuations. Figure 4(b) plots  $\Delta\varphi(t)$  of the measured FMCW signals based on employing Hilbert transform on the time series at the oscilloscope over

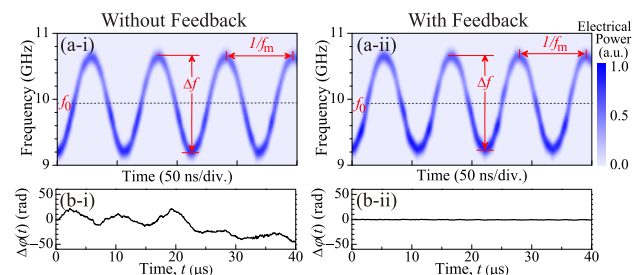


**Fig. 4.** (a) Spectrogram and (b) phase deviation  $\Delta\varphi(t)$  of the FMCW emission generated from the slave laser under modulated optical injection. The feedback from PD2 to MZM is (i) disconnected and (ii) connected.

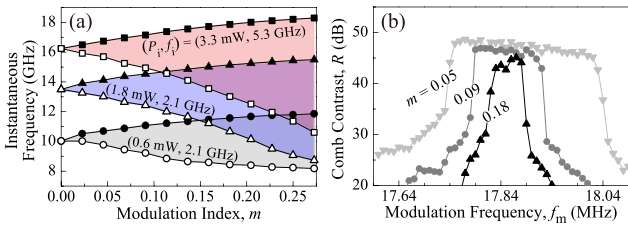


**Fig. 5.** (a) Range of the instantaneous frequency sweep as a function of  $m$  at different  $(P_i, f_i)$ . The closed and open symbols show the maximal and minimal instantaneous frequencies  $f_0 \pm \Delta f/2$ , respectively. (b) Frequency comb contrast  $R$  as a function of  $f_m$  at different  $m$ .

a long duration of 40  $\mu$ s in Fig. 4(b) [12]. For Fig. 4(b-i) without feedback, the FMCW signal is noisy in having  $\Delta\varphi(t)$ , which significantly fluctuates over time. The fluctuation implies imperfect repeatability of the FMCW signals across different cycles of  $1/f_m$ , which explains the broad linewidths of the frequency comb components in Fig. 3(c-i). As for Fig. 4(b-ii) with feedback, the phase noise is much reduced with  $\Delta\varphi(t)$  staying well within  $\pm\pi/4$  even over a long duration exceeding  $10^3$  cycles of  $1/f_m$ . The reduction of the fluctuations of  $\Delta\varphi(t)$  is consistent with the narrow linewidths and large contrast of the frequency comb in Fig. 3(c-ii). The phase noise reduction is achieved because the feedback signal is delayed by  $\tau = 1/f_m$  which is exactly one cycle of the frequency modulation of the P1 oscillation of the slave laser. Thus the instantaneous microwave frequency of the P1 oscillation always matches that of the feedback at the slave laser for suppressing phase fluctuations.

The tunability of the P1 dynamics allows the tuning of  $f_0$  as well as  $\Delta f$  for the FMCW signal, as shown in Fig. 5(a), where circles, triangles, and squares correspond to  $(P_i, f_i) = (0.6 \text{ mW}, 2.1 \text{ GHz})$ ,  $(1.8 \text{ mW}, 2.1 \text{ GHz})$ , and  $(3.3 \text{ mW}, 5.3 \text{ GHz})$ , respectively. Generally, increasing  $P_i$  and  $f_i$  leads to increasing  $f_0$  [15,22]. For instance, at  $m = 0$ , changing  $P_i$  from 0.6 to 3.3 mW results in increasing  $f_0$  from 10 to 16 GHz, which exceeds twice the relaxation resonance frequency of the slave laser. The sweep range  $\Delta f$  varies with  $(P_i, f_i)$  even when  $m$  is fixed due to the variation of the sensitivity of  $f_0$  on the injection power [25]. Also, when  $(P_i, f_i)$  are fixed, the sweep range  $\Delta f$  increases with  $m$ . The instantaneous frequency sweeps within a shaded region bounded by the maximum  $f_0 + \Delta f/2$  and the minimum  $f_0 - \Delta f/2$  in closed and open symbols, respectively. The sweep range  $\Delta f$  reaches 7.7 GHz at  $m = 0.27$ , corresponding to a maximal FMCW frequency sweep rate of  $\pi\Delta f f_m = 0.42 \text{ GHz/ns}$ , for the squares in Fig. 5(a).

The stability of the FMCW signal is quantified by the frequency comb contrast  $R$  in Fig. 5(b), as the external modulation frequency  $f_m$  is tuned around  $1/\tau = 17.84 \text{ MHz}$ . Fixing  $(P_i, f_i)$  at  $(0.6 \text{ mW}, 2.1 \text{ GHz})$ , the modulation index  $m$  is set at 0.05, 0.09, and 0.18 for the down-triangles, circles, and up-triangles, respectively. When  $f_m$  is exactly  $1/\tau$ , the comb contrast  $R$  is always greater than 40 dB because of the locking of the optoelectronic cavity modes in giving a stable FMCW signal with reduced phase noise. When  $f_m$  is tuned away from  $1/\tau$ ,  $R$  drastically drops by over 20 dB because the modes are no longer locked. As  $m$  increases, the locking range of  $f_m$  for  $R > 40 \text{ dB}$  reduces due to the increasing difficulty to lock an increasing number of modes within  $\Delta f$  for stable FMCW generation.

In summary, modulation on the P1 oscillation of the optically injected semiconductor laser is utilized for FMCW microwave generation, where the central frequency is widely tunable beyond the relaxation resonance frequency, and the sweep range is dependent on the modulation index. Phase noise reduction of the FMCW signal is also illustrated through feedback stabilization. An improvement of the frequency comb contrast by 30 dB, a sweep range reaching 7.7 GHz, and a sweep rate of up to 0.42 GHz/ns illustrate the use of P1 oscillation in FMCW generation.

**Funding.** Research Grants Council of Hong Kong, China (CityU 111213, CityU 11201014).

## REFERENCES

- J. Capmany and D. Novak, *Nat. Photonics* **1**, 319 (2007).
- J. P. Yao, *J. Lightwave Technol.* **27**, 314 (2009).
- L. F. Lester, N. A. Naderi, F. Grillot, R. Raghunathan, and V. Kovanis, *Opt. Express* **22**, 7222 (2014).
- T. B. Simpson, J. M. Liu, M. AIMulla, N. G. Usechak, and V. Kovanis, *Phys. Rev. Lett.* **112**, 023901 (2014).
- T. B. Simpson, J. M. Liu, M. AIMulla, N. G. Usechak, and V. Kovanis, *IEEE J. Sel. Top. Quantum Electron.* **19**, 1500807 (2013).
- A. Kanno and T. Kawanishi, *J. Lightwave Technol.* **32**, 3566 (2014).
- W. F. Zhang and J. P. Yao, *J. Lightwave Technol.* **34**, 4664 (2016).
- J. McKinney, D. Leaird, and A. Weiner, *Opt. Lett.* **27**, 1345 (2002).
- W. Zou, H. Zhang, X. Long, S. Zhang, Y. Cui, and J. Chen, *Sci. Rep.* **6**, 19786 (2016).
- S. Gao and R. Hui, *Opt. Lett.* **37**, 2022 (2012).
- G. Pyo, J. Yang, C. Y. Kim, and S. Hong, *IEEE Trans. Circuits Syst. II, Exp. Briefs* **61**, 393 (2014).
- F. Wei, B. Lu, J. Wang, D. Xu, Z. Pan, D. Chen, H. Cai, and R. Qu, *Opt. Express* **23**, 4970 (2015).
- J. W. Shi, F. M. Kuo, N. W. Chen, S. Y. Set, C. B. Huang, and J. E. Bowers, *IEEE Photon. J.* **4**, 215 (2012).
- Y. Tong, Q. Zhou, D. Han, B. Li, W. Xie, Z. Liu, J. Qin, X. Wang, Y. Dong, and W. Hu, *Opt. Lett.* **41**, 3787 (2016).
- S. C. Chan, S. K. Hwang, and J. M. Liu, *Opt. Express* **15**, 14921 (2007).
- S. C. Chan, *IEEE J. Quantum Electron.* **46**, 421 (2010).
- Y. S. Juan and F. Y. Lin, *IEEE Photon. J.* **3**, 644 (2011).
- Y. Wang, J. Zheng, M. Zhang, and A. Wang, *IEEE Photon. Technol. Lett.* **23**, 158 (2011).
- A. Hurtado, I. D. Henning, M. J. Adams, and L. F. Lester, *Appl. Phys. Lett.* **102**, 201117 (2013).
- P. Perez, A. Quirce, A. Valle, A. Consoli, I. Noriega, L. Pesquera, and I. Esquivias, *IEEE Photon. J.* **7**, 1 (2015).
- L. Fan, G. Xia, J. Chen, X. Tang, Q. Liang, and Z. Wu, *Opt. Express* **24**, 18252 (2016).
- J. P. Zhuang and S. C. Chan, *Opt. Lett.* **38**, 344 (2013).
- C. Wang, R. Raghunathan, K. Schires, S. C. Chan, L. F. Lester, and F. Grillot, *Opt. Lett.* **41**, 1153 (2016).
- K. L. Hsieh, Y. H. Hung, S. K. Hwang, and C. C. Lin, *Opt. Express* **24**, 9854 (2016).
- J. P. Zhuang and S. C. Chan, *Opt. Express* **23**, 2777 (2015).
- S. C. Chan and J. M. Liu, *IEEE J. Sel. Top. Quantum Electron.* **10**, 1025 (2004).
- C. Cui, X. Fu, and S. C. Chan, *Opt. Lett.* **34**, 3821 (2009).
- C. H. Chu, S. L. Lin, S. C. Chan, and S. K. Hwang, *IEEE J. Quantum Electron.* **48**, 1389 (2012).
- S. C. Chan and J. M. Liu, *IEEE J. Quantum Electron.* **41**, 1142 (2005).
- Y. H. Hung and S. K. Hwang, *Opt. Lett.* **38**, 3355 (2013).
- J. P. Zhuang, X. Z. Li, S. S. Li, and S. C. Chan, in *Asia Communications and Photonics Conference* (2015), paper ASu5I-2.
- M. Brunel and M. Vallet, *Opt. Lett.* **33**, 2524 (2008).
- P. Zhou, F. Zhang, B. Gao, and S. Pan, *IEEE Photon. Technol. Lett.* **28**, 1827 (2016).
- R. Huber, M. Wojtkowski, and J. Fujimoto, *Opt. Express* **14**, 3225 (2006).